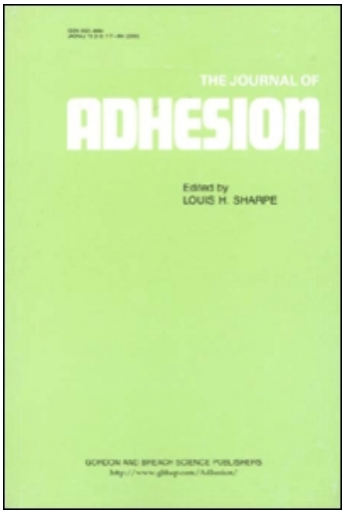

The Journal of Adhesion
Publication details, including instructions for authors and subscription information:
http://www.informaworld.com/smpp/title~content=t713453635

Surface Energetics and Adhesion

Tennyson Smith[a]
[a] Rockwell International Science Center, Thousand Oaks, California, U.S.A.

To cite this Article Smith, Tennyson(1980) 'Surface Energetics and Adhesion', The Journal of Adhesion, 11: 3, 243 — 256
To link to this Article: DOI: 10.1080/00218468008078920
URL: http://dx.doi.org/10.1080/00218468008078920

J. Adhesion, 1980, Vol. 11, pp. 243–256
0021-8464/80/1103-0243 $06.50/0

Printed in Great Britain

Surface Energetics and Adhesion†

TENNYSON SMITH

Rockwell International Science Center, Thousand Oaks, California 91360, U.S.A.

(*Received February 12, 1980; in final form August 25, 1980*)

The relationships between surface energetics and adhesion are critically reviewed. New data that confirm such relationships, for peel tests as well as lap shear tests, are presented. The effect of hydrothermal aging of aluminum surfaces on surface energetics can be used to predict degradation in bond strength. The mechanism of failure for elastic adhesives (such as Scotch ® tape) in peel tests may be essentially the same as for more brittle adhesives (such as epoxies) in lap shear tests. This mechanism may involve brittle fracture that forms a critical flaw at the adherend-adhesive interface (on a microscopic level), followed by crack propagation which then may include considerable elastic and plastic deformation. The locus of propagation (fractography) is generally not (but may be) relevant to the problem of how to remedy mechanical weakness in an adhesive joint, since the local region of critical flaw formation rather than the general surface area determines the joint strength.

INTRODUCTION

A review of relationships between surface energetics and bond strength has been given by Mittal.[1] He states: "It is universally agreed that practical adhesion cannot be equated with thermodynamic adhesion; at most, one can expect a direct correlation between the two." According to Mittal, when adhesives exhibit finite contact angles there is a direct correlation between work of adhesion and bond strength. He states also, that when adhesives completely wet the adherends, strengths increase with increasing work of adhesion going through maxima at minimum values of interfacial tension.

Numerous studies have shown the above mentioned correlations between surface energetics and practical adhesion; however, there are studies for

† Presented at the Annual Meeting of the Adhesion Society, Savannah, Ga, U.S.A., February 10–13, 1980.

which no correlation exists and theoretical reason not to expect such a correlation. This is particularly true when joint failure is not at the adhesive-adherend interface.

This paper presents new experimental data that does correlate surface energetics and practical adhesion, discusses theoretical expectations, and presents a possible explanation for why correlations exist even for joints that fail primarily by cohesive rather than adhesive failure.

Surface energetics analysis (SEA)

According to Kaelble[2,3] the general concept for regular adsorption bonding of interfaces is summarized in the following relation for interfacial tension:

$$\gamma_{ij} = (\alpha_i - \alpha_j)^2 + (\beta_i - \beta_j)^2 + \Delta_{ij} \tag{1}$$

where the parameters are defined in Table 1 and subscripts denote interactions between phase i and j. Interfaces dominated by Van der Waal's interactions are termed regular interfaces, and the value of the excess term Δ_{ij} of Eq. (1) which describes interdiffusion or ionic-covalent interactions can be considered negligible. This is a much more general case than one might expect and permits application of surface energy analysis to a wide range of materials. When $\Delta_{ij} = 0$, Eq. (1) defines an ideal interface with $\gamma_{ij} = 0$ as the special case where $\alpha_i = \alpha_j$ and $\beta_i = \beta_j$.

The special combination of surface energy and fracture mechanics parameters that enter the modified Griffith relation are defined in Table II; they show that the Griffith fracture energy, γ_G, is defined by the following relation:

$$\gamma_G = -(1/2)S_2 = R^2 - R_0^2. \tag{2}$$

A circular parabola in γ_G, α_2, β_2 Cartesian space is defined by Eq. (2). The surface energies α_2 and β_2 for the immersion phase 2 which provide the condition $R < R_0$, result in the spreading coefficient $S_2 > 0$ for phase 2. The predicted consequence for $S_2 > 0$ is that phase 2 should spontaneously debond phase 1 from phase 3 in the absence of rheological constraints. When $R > R_0$, the Griffith fracture energy becomes positive and a critical mechanical stress, σ_c, which depends on γ_G (see Table II), is now required for crack extension.

The relations in Table I and Table II form the basis for designed experiments that isolate the discrete mechanisms of polar and dispersion interactions across the interface. The test liquids display a wide range of polar character in surface tension, with $\beta_l/\alpha_l = 1.53$ for water to $\beta_l/\alpha_l = 0$ for linear hydrocarbons. Inspection of Eq. (*e*) in Table I shows that by using measured values of work of adhesion, W_a, by contact angle measurements

TABLE I

Surface energetics relations

$$\gamma_{LV} = \gamma_{LV}^d + \gamma_{LV}^p = \alpha_L^2 + \beta_L^2 \quad (a)$$

$$\gamma_{SV} = \gamma_{SV}^d + \gamma_{SV}^p = \alpha_S^2 + \beta_S^2 \quad (b)$$

$$W_a = \gamma_{LV}(1 + \cos\theta) \leqslant 2\gamma_{LV} \quad (c)$$

$$W_a = 2[\alpha_L \alpha_S + \beta_L \beta_S] \quad (d)$$

$$\frac{W_a}{2\alpha_L} = \alpha_S + \beta_S(\beta_L/\alpha_L) \quad (e)$$

$$\frac{W_a}{2\alpha_S} = \alpha_L + \beta_L(\beta_S/\alpha_S) \quad (f)$$

where: γ_{LV} = liquid-vapor tension; γ_{SV} = solid-vapor surface tension; α_L, β_L = square root of the respective (London) dispersion γ_{LV}^d and (Keesom) polar γ_{LV}^p; α_S, β_S = square roots of respective dispersion γ_{SV}^d and polar γ_{SV}^p; W_a = nominal work of adhesion; θ = liquid-solid contact angle.

for liquids of known α_l and β_l, isolation of the solid-vapour surface properties α_s and β_s is permitted. The intercept of the plot of $W_a/2\alpha_l$ versus β_l/α_l isolates α_s as the intercept and β_s as the slope.

Measurement of α and β suffers from the same problem as measurement of critical surface tension (of Zisman): values of α and β depend on the fluids used to make the measurement. By using a consistent set of fluids, it is hoped that meaningful relative values will result.

Experimental tests of SEA

Advantages of Kaelble's SEA are the simple diagrammatical form of presenting the data and the ease of interpretation of the data. Figure 1 shows SEA diagrams which are used to test SEA for real systems. As previously described, the dispersion (α) and polar (β) nature of solid surfaces can be obtained from plots of $W_a/2\alpha_L$ versus β_L/α_L for liquids of known α and β character. The work of adhesion, W_a, is determined from the surface tension, γ_{LV}, and contact angle, θ, of the liquid on the solid [*i.e.*, $W_a = \gamma_{LV}(1 + \cos\theta)$].

A circle of radius R_0 (Figure 1*b*) is drawn so that it passes through the α, β coordinates of phases 1 and 3; in this case, phase 1 is silicone tape and phase 3 is a clean microscope slide. As might be expected, the adhesive tape has little polar character and the glass slide has polar character approaching that of water. Air has no dispersion or polar character ($\alpha_{air} = 0$, $\beta_{air} = 0$). R is the vector from the center of the circle to the α, β coordinates of phase 2. According to Table II, if $R < R_0$, the critical stress needed to separate

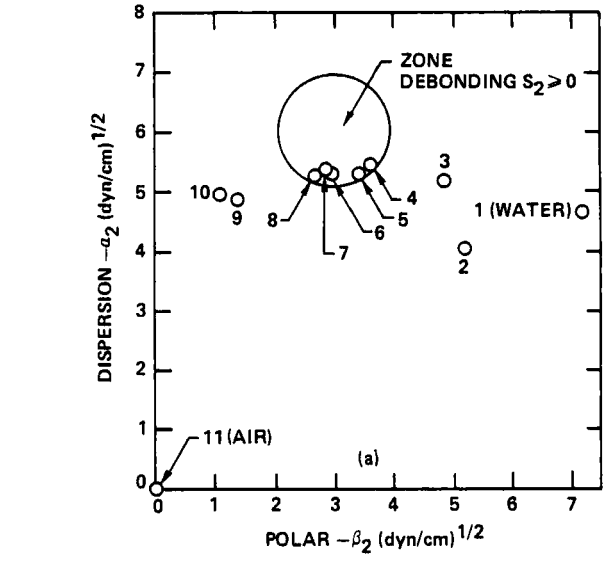

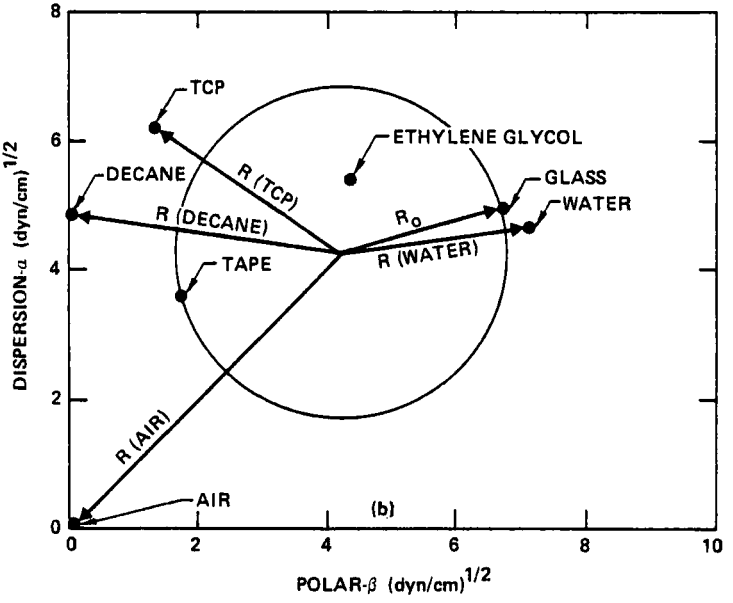

FIGURE 1 Surface energetics diagram pPr/pvCl$_2$ (*a*), tape/glass (*b*) with various immersion fluids.

TABLE II

Fracture mechanics relations

$$\sigma_c = \left(\frac{2E\gamma_G}{\pi C}\right)^{1/2} = \left(\frac{2E}{\pi C}\right)^{1/2} (R^2 - R_0^2)^{1/2} \geqslant 0 \qquad (a)$$

$$\gamma_G = R^2 - R_0^2 \qquad (b)$$

$$R_0^2 = 0.25[(\alpha_1 - \alpha_3)^2 + (\beta_1 - \beta_3)^2] \qquad (c)$$

$$R^2 = (\alpha_2 - H)^2 + (\beta_2 - K)^2 \qquad (d)$$

$$H = 0.5(\alpha_1 + \alpha^3) \qquad (e)$$

$$K = 0.5(\beta_1 + \beta_3) \qquad (f)$$

where σ_c = critical crack propagation stress; γ_G = Griffith surface energy for fracture; E = Young's modulus; C = crack length; α_1, β_1 = surface properties of adhesive phase 1; α_2, β_2 = surface properties of environment phase 2; α_3, β_3 = surface properties of adherend, phase 3.

phase 1 from 3 is zero, *i.e.*, the circle is the boundary of spontaneous debonding of phase 1 from phase 3. If $R > R_0$, some fracture energy is needed to separate phase 1 from phase 3.

Since Eq. (*a*) in Table II is limited to brittle fracture, does not consider plastic deformation, and has unknown quantities such as crack length C, one cannot expect to predict the absolute critical stress σ_c with it. However, there is hope that the effect of phase 2 (air, water, etc.) might be revealed by comparing the ratio of $\sigma_{c_2}/\sigma_{c_{air}}$, as calculated from

$$(R_2^2 - R_0^2)^{1/2}/(R_{air}^2 - R_0^2)^{1/2},$$

with the ratio of the peel energy W required to strip the tape in phase 2 versus that required in air.

Spontaneous debond

To test the spontaneous debonding relationships, Kaelble[2] calculated the α, β parameters from the results of Owens[4] and plotted the data as in Figure 1*a*. Those solutions (4–8) with α_2, β_2 coordinates that fall within the circle caused spontaneous debonding (in <15 min) of flamed polypropylene (Pr) (phase 1) from a thin layer of poly (vinylidene chloride) ($pvCl_2$) copolymer (phase 3), whereas those solutions (1, 2, 3, 9, 10) with coordinates outside the circle did not cause debonding in six months immersion. On the other hand, Figure 1*b* is a SEA diagram for experiments by the author. Scotch tape (ordinary 3M office tape) bonded to a clean glass microscope slide was immersed in ethylene glycol, which (according to Figure 1*b*) should spon-

taneously debond the tape from the glass. In 72 hours there was no spontaneous debonding, in contradiction to the prediction. This result is perhaps due to forces between the tape and glass that are not measured by the SEA technique, *e.g.*, acid-base or other chemical bonds. It may also be that this higher energy glass surface adsorbs species that will affect SEA in a way different from the actual interaction between adhesive and glass, *i.e.*, the excess term in Eq. (1) cannot be neglected.

Peel tests

Table III gives the α, β and calculated R_0^2 and R^2 values for the tape-glass, tape-Nylon (6-6) and tape-Kapton systems. The α, β coordinates and R vectors are plotted in Figure 1*b*. Phase 2 (water, n-decane, tricresylphosphate (TCP), and air) all fall outside the circle. The predicted force needed to peel the tape (proportional to σ_c^2) from the glass should decrease in the order, air, n-decane, TCP and water. Although W for TCP is high the predicted decrease with respect to air is observed in every case. The liquids may change the physical properties of the tape adhesive which will, in turn, affect the peel values. For example, the high peel force with TCP may be due to TCP softening of the adhesive so that it absorbs more energy in the peel process. Since other parameters, such as the crack length C and effective modulus of elasticity E, are different for different systems, correlation of all the systems is not expected. If phase 2 does not change the adhesive, correlation may be expected for a given set of phase 1 and 3 but differing phase 2. The right hand columns of Table III report the ratio of $\gamma_G/\gamma_{G\ \mathrm{air}}$ and W_2/W_{air}, respectively. By computing the ratio of the surface energetics calculation of the γ_G to that in air, it is hoped that mechanical effects will cancel. There is a surprisingly good correlation between the SEA predictions and the measured peel force ratios (W_2/W_{air}).

A similar correlation is observed for the data of Gent and Schultz[5] if γ_G is calculated from Table IV of Reference 2. They performed a T peel between a crosslinked elastomer (60/40 butadiene/styrene copolymer) and a polyester. The rate of peel was 1 cm/s at 23°C.

Figure 2 (solid dots) is a plot of the work of peel W versus the water contact angle prior to bonding Scotch tape to aluminum alloy that had been contaminated to differing levels. In many instances a plot of β versus θ_{H_2O} reveals a direct correlation, with β decreasing linearly with increasing θ_{H_2O}. The decrease in W with increasing θ_{H_2O} in Figure 2 corresponds to a decrease in β and therefore γ_G. Although there is considerable scatter, there is a correlation between work of peel and surface energetics.

One might expect that if a correlation exists between W and surface energetics, failure must be adhesive rather than cohesive. However, another

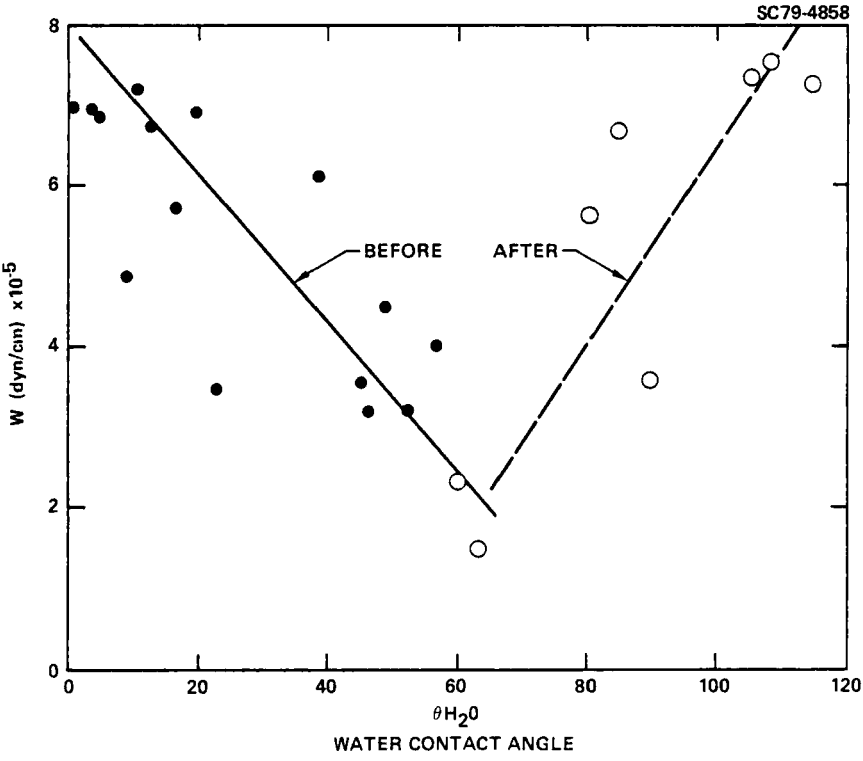

FIGURE 2 Plot of peel work versus water contact angle (θ_{H_2O}). The contact angle was measured prior to peel for one set (●) and after peel for another set (○). Sample surface energy was varied by different contamination levels.

set of specimens was peeled and the water contact angle was measured after peel. The open circles in Figure 2 show the result, the contact angle after peel increases with increasing W. In spite of the correlation between W and surface energetics there is increasing adhesive transfer (cohesive failure) with increasing peel strength. A hypothesis for this is described later.

Lap shear tests

Correlations similar to those in the right hand column of Table III for peel tests have been observed by Smith and Kaelble[6] for the effect of humidity aging on the lap shear strength of aluminium alloys bonded with modified epoxy adhesives (HT424 from American Cyanamide). This may be due to a similar fracture mechanism as is discussed later.

After an FPL (H_2SO_4-dichromate) etch, the aluminum samples were exposed to 95% RH, 54°C in a humidity chamber for various lengths of time.

Table III

Comparison of surface energetics analysis with peel tests for Scotch tape on glass, Nylon and Kapton†

Phase 1 α_1	β_1	Phase 2 α_2	β_2	Phase 3 α_3	β_3	R_0^2	R^2	γ_G	W_{peel} (dyn/cm) $\times 10^{-4}$	$\gamma_G/\gamma_{G\,air}$	W_2/W_{air}
Scotch tape		Air		*Glass*							
3.6	1.7	0	0	4.96	6.72	6.76	36.0	29.20	28.4±2.7	1.0	1.0
		Decane									
		4.89	0			6.76	18.1	11.30	18.0±2.7	0.4	0.6
		TCP									
		6.26	1.30			6.76	12.4	5.64	21.3±2.4	0.2	0.7
		Water									
		4.67	7.14			6.76	8.7	2.00	1.2±0.3	0.07	0.04
		Air		*Nylon 6-6*							
		0	0	5.21	5.22	3.74	31.4	27.6	39.3±2.1	1.0	1.0
		Water									
		4.67	7.14			3.74	13.6	9.9	17.2±2.1	0.4	0.4
		Air		*Kapton*							
		0	0	5.54	4.28	2.60	29.8	27.2	12.4±1.0	1.0	1.0
		Water									
		4.67	7.14			2.60	17.2	14.6	9.8±0.6	0.5	0.8

† Glass thickness 0.3 cm, Nylon thickness 0.06 cm, Kapton thickness 0.016 cm, peel rate 0.25 cm/s at 23°C.

Figure 3 shows the drift of the surface energetics parameters, α to higher values and β to lower values. The ratio of $\sqrt{\gamma_G}$ after humidity aging to that of $\sqrt{\gamma_G}$ dry was calculated from the α, β parameters. According to Eq. (*a*) in Table II, this ratio should be approximately equal to the ratio of the theoretical lap shear strengths. Measurements of the actual lap shear strengths after various surface exposure times (SET) and after bond exposure times (BET) are reported in Figure 4. The ratio of the measured values of σ wet to σ dry of 0.69 is in close agreement with the predicted value of 0.64 from SEA (see Table IV). It is of interest to note that, as for the peel tests in Figure 2, the aluminum lap shear joints failed with considerable cohesive failure (*i.e.*, 40–60%), even though surface energetics for adhesive failure seems to apply.

Similar experiments were performed for titanium, 6% Al, 4% V, alloy, (Ti 6Al4V) with HT 424 adhesive. After 20 hours SET, $\sqrt{\gamma_{G\,wet}}/\sqrt{\gamma_{G\,dry}}$ proved to be 0.84, compared to the measured value of 0.95. The correlation is not as good because, for titanium, the failure was more cohesive (within the HT 424 adhesive) than for aluminum. Measurements of the β parameter of the adhesive before and after humidity aging (1000 hour BET) allowed the

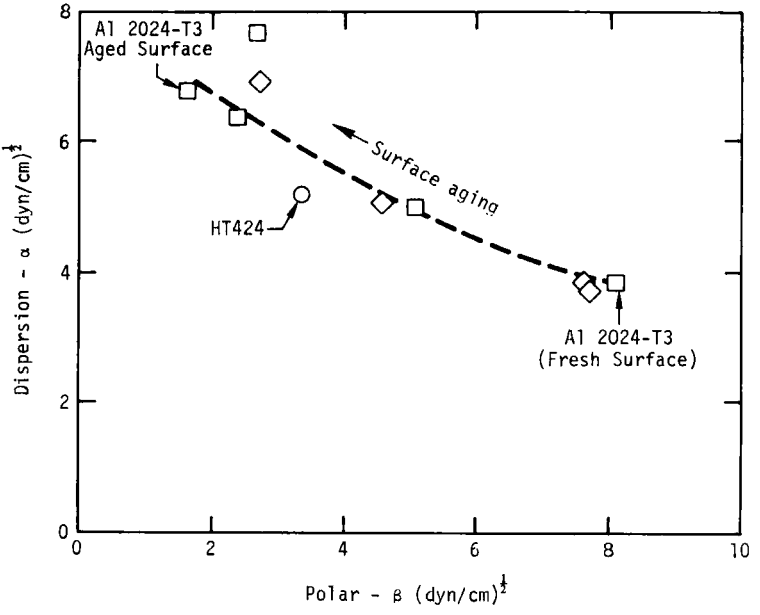

FIGURE 3 Surface energetics plot of α versus β for hydrothermal aging (SET) at 95% RH, 54°C of Al2024-T3.

calculation of $\sqrt{\gamma_{G\,wet}}/\sqrt{\gamma_{G\,dry}}$, for cohesive failure, of 0.63. This is in excellent agreement with the measured lap shear ratio of 0.64 for cohesive failure (for which phases 1 and 3 are the same). These results give further evidence of a correlation between practical adhesive strengths and surface energetics.

DISCUSSION

Except for the failure of ethylene glycol to debond Scotch tape spontaneously from glass and some deviations from quantitative expected values of the effect of phase 2 on peel and lap shear strength, there seems to be a definite correlation between bond strength, bond durability under hydrothermal stress, and surface energetics. However, as discussed next, there has been controversy in the literature as to whether such a correlation should exist.

Weak boundary layer

Bikerman has continued[7,8] to argue that for a "proper joint", true interfacial failure practically never occurs. He proposed the "weak boundary layer" (WBL) theory for what generally appears to be interfacial failure. His argu-

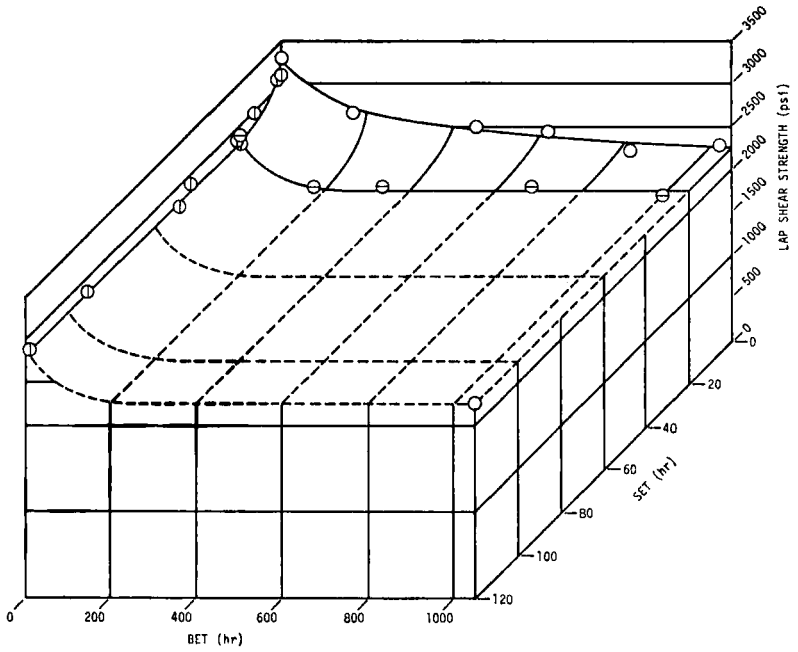

FIGURE 4 SET, BET diagram, of lap shear strengths for Al2024-T3/HT424 after aging at 95% RH, 54°C.

ment is based on the concept that if two phases are adhering, the cohesive strength of one will be greater than the other and the strength of adhesion will be something between that for the cohesive strength of the phases; therefore, failure will occur in the weaker phase and not at the interface. If a weak boundary layer is present, failure will occur in this weakest phase. Bikerman also argues that the probability of crack propagation along the interfacial plane is extremely small considering the possible alternative directions after each step forward.

Good[9] gives convincing arguments to refute the arguments presented by Bikerman, but he does not reject the principle for failure of a considerable percentage of practical adhesive joints. Weak boundary layers consist of organic contamination, weak oxides or hydroxides. Solid polymer may have low molecular weight materials such as plasticizers or antioxidant molecules, or if it is crystalline the surface material may be amorphous, etc. If failure never occurs at the interface, one can expect no relation between surface energetics and practical adhesive strengths. On the other hand, if a weak boundary layer exists, it is likely to be reflected in surface energetics prior to bonding.

TABLE IV

Comparison of the ratio predicted from SEA (*i.e.*, $\sqrt{\gamma_{G\,wet}}/\sqrt{\gamma_{G\,dry}}$), to the measured lap shear values

System	Lap shear strength ratios Predicted ($\sqrt{\gamma_{G\,wet}}/\sqrt{\gamma_{G\,dry}}$)	Measured σ wet/σ dry
Al 2024-T3/HT424		
95% RH, 54°C		
SET 120 hour, BET 1000 hour	0.64	0.69
Ti 6Al4V/HT 424		
95% RH, 54°C		
SET 20 hour	0.84	0.95
BET 1000 hour	0.63	0.64

Molecular contact

Huntsberger[10] emphasizes that the primary effect on adhesion is wetting, either as an equilibrium process or as a rate process. Calculations indicate that if one-to-one interaction between molecules is inhibited, the attractive forces can be greatly reduced. Intermolecular contact can be limited by molecular size, chain configuration (polymers) and orientation if equilibrium is attained. If thermodynamic equilibrium is achieved, Huntsberger points out that good adhesion may not be limited to surfaces that exhibit zero or low contact angles, because if the contact angle is less than 90°, equilibrium will induce complete wetting. Since the contact angle is usually $<90°$, only rarely would the interfacial free energy (surface energetics) establish the extent of wetting and thus bonding.

If thermodynamic equilibrium is not achieved, molecular contact will be limited by rate processes such as spreading and dissolution of trapped air. On high energy surfaces, the higher surface tension liquids will have higher capillary pressure and consequently maximum wetting rates. Air entrapment diminishes wetting rate and might preclude wetting on a macroscopic scale. On a microscopic scale, high pressure and solubility results in liquid absorption of trapped gas in the fluid and more rapid spreading. Although other parameters (*e.g.*, fluid viscosity) are involved, the rate of wetting is related to surface energetics and thus for non-equilibrium one might expect some correlation between SEA and bond strength.

More than one component

If the adhesive contains more than one component, selective adsorption from solution can change surface properties and influence wetting. Two phases

with different viscosity can fill interstices with the more fluid phase even though the more viscous phase might wet. As solvent evaporates, if the glass transition temperature has not been reached (a cooling, before wetting is complete), evaporation will cause stresses concentrated at edges of non-wetted interstices and may cause separation or weaken the bond. In the first instance SEA would be involved, in the second and third instances SEA may not be involved in the bond strength.

Huntsberger[10] makes the point that more strongly interacting groups (coupling agents) or bonding stronger than Van der Waals, only affect joint performance in two ways:

1) changes in contact density, and
2) changes in energy state to increase or decrease wetting.

Both of these mechanisms might be reflected in SEA.

Plastic deformation work

As indicated above, it has generally been demonstrated that surface energetics should be involved in adhesion, but there is one aspect of Eq. (*a*), Table II that has not been considered. The work expended in fracturing a solid involves plastic deformation energy as well as the energy γ_G to separate two surfaces. Experimental and theoretical analysis indicate that except for extremely brittle solids (*e.g.*, glass, ceramics, etc.) the plastic term is orders of magnitude larger than the surface energy term. Since the energy terms are additive, the surface energy term is negligible and there should be no correlation between surface energetics and bond strength. Since there is a correlation between SEA and bond strength, Kaelble[1] concluded that the plastic work, W_p, is a direct function of γ_G. The answer to this paradox may be found in an analysis of the locus of failure.

Locus of failure

Huntsberger[10] states, "The most fruitful avenue of research for solution of the adhesion problem can be selected only on the basis of unequivocal establishment of the locus of failure." Good[9] and Andrews[11] point out that "the initiation and the propagation of fracture in a solid or two phase adhering joint, are two different problems. The question of the locus of propagation is not in general directly relevant to the problem of how to remedy mechanical weakness in an adhering system". This author[12] has pointed out that the locus of crack initiation is of primary interest.

Although one might think that a bond that fails with apparent cohesive or partial cohesive fracture, as observed for peel tests and also for the lap shear

aging studies for aluminum, would show relationships to bulk properties and would not be related to surface energetics, this may not be true for the reasons indicated below.

The locus of failure initiation can be all important and will not necessarily be in the same plane throughout the bonded joint. As a consequence, fractography after bond failure can be misleading.

It has been shown[12] in the case of lap shear joints, between Al7075-T6 with a modified epoxy with a nylon scrim (FM73 for American Cyanamide), that the lap shear strength can be directly related to the fraction of the bond area that failed at the metal-adhesive interface. This was because the deliberate contamination of the adherends, to provide weak boundary layers, was fairly uniform over the surface. It is quite probable that in some cases a weak interfacial layer would not be uniform. In this case the region of critical flaw formation could be a minute spot of contaminated surface. The result might be that, although crack initiation would occur at the weak boundary layer spot, crack propagation would deviate from the surface into the bulk adhesive. Fractographic analysis would be interpreted as cohesive failure in the bulk adhesive, when in fact the fracture strength was governed by the surfaced properties of the unobserved critical flaw region.

The point is that even though fracture may be interpreted as cohesive failure it may be directly related to the surface in the critical flaw region and thus in some instances to surface energetics. However, the surface energetics would be that of the contaminated spot and would have to be measured at that spot, in order to correlate surface energetics with bond strength.

CONCLUSIONS

For theoretical and experimental reasons, one should expect a correlation between surface energetics measured prior to adhesive bonding and bond strength and hydrothermal stress endurance after bonding. However, this expectation must be used with caution since there are situations for which other nonthermodynamic parameters control resultant bond strength.

Fractography of a fractured bond reveals the path of least resistance during crack propagation but may give no indication of crack initiation and therefore, joint strength. However, in many instances, if surface defects that initiate critical flaws are uniformly distributed in the joint, fractography will reveal information about the initiation process. Thus the observation that cohesive fracture has occurred does not rule out that the critical flaw was formed at the interface and was directly related to surface energetics. Examination of fracture surfaces with sophisticated surface tools such as ESCA, AES

and SIMS, etc., may be misleading, with respect to the mechanism of failure, unless the critical flaw region is examined.

Finally, there is no reason to invoke a direct functionality between the plastic work W_p and γ_G because failure is initiated at the critical flaw region and the critical flaw may form because of its brittle nature, even for the adhesive on Scotch tape, for which the bulk of the joint may be very elastic and plastic in nature. The brittle nature results from the rate of strain in the deformed layer being very high so that viscous deformation is suppressed.

The mechanism of failure for elastic adhesives (such as on Scotch tape) in peel tests, may be essentially the same as for more brittle adhesives (such as epoxies) in lap shear tests. This mechanism may involve brittle fracture to form a critical flaw at the adherend-adhesive interface, followed by crack propagation, which may include considerable plastic deformation. The locus of propagation (fractography) is generally not (but may be) relevant to the problem of how to remedy mechanical weakness in an adhesive joint, since the region of critical flaw formation determines joint strength.

References

1. K. L. Mittal, in *Adhesion Science and Technology*, L.-H. Lee, Ed. (Polymer Science and Technology Series, **9A**, Plenum, N.Y., 1975), p. 129.
2. D. H. Kaelble, *J. Appl. Polym. Sci.* **18**, 1869 (1974).
3. D. H. Kaelble, *J. Adhesion* **2**, 66 (1970).
4. D. K. Owens, *J. Appl. Polym. Sci.* **14**, 1725 (1970).
5. A. N. Gent and J. Schultz, *J. Adhesion* **3**, 281 (1972).
6. T. Smith and D. H. Kaelble, "Mechanism of Adhesion Failure Between Polymers and Metallic Substrates", Air Force Materials Laboratory Tech. Report: AFML-TR-74-73, June 1974.
7. J. J. Bikerman, *J. Coll. Sci.* **2**, 163 (1947).
8. J. J. Bikerman, *The Science of Adhesive Joints*, 2nd Ed. (Academic Press, N.Y., 1968).
9. R. J. Good, *J. Adhesion* **4**, 133 (1972).
10. J. R. Huntsberger, in *Treatise on Adhesion and Adhesives*, *Vol. 1*, R. L. Patrick, Ed. (Marcel Dekker Inc., New York, 1967), p. 119.
11. E. H. Andrews, *Fracture in Polymers* (Oliver and Boyd, London, 1968).
12. T. Smith and P. Smith, in *Adhesion and Adsorption of Polymers*, L.-H. Lee, Ed. (Polymer Science and Technology Series, **12A**, Plenum, N.Y., 1980).